

Neutralino dark matter and Higgs mediated lepton flavor violation in the minimal supersymmetric standard model

M. Cannoni¹ and O. Panella²

¹*Università di Perugia, Dipartimento di Fisica, Via A. Pascoli, 06123, Perugia, Italy*

²*Istituto Nazionale di Fisica Nucleare, Sezione di Perugia, Via A. Pascoli, 06123 Perugia, Italy*

(Dated: December 22, 2018)

We re-examine the prospects for the detection of Higgs mediated lepton flavor violation at LHC, at a photon collider and in τ decays such as $\tau \rightarrow \mu\eta$, $\tau \rightarrow \mu\gamma$. We allow for the presence of a large, model independent, source of lepton flavor violation in the slepton mass matrix in the $\tau - \mu$ sector by the mass insertion approximation and constrain the parameter space using the τ LFV decays together with the B -mesons physics observables, the anomalous magnetic moment of the muon and the dark matter relic density. We further impose the exclusion limit on spin-independent neutralino-nucleon scattering from CDMS and the CDF limits from direct search of the heavy neutral Higgs at the TEVATRON. We find rates probably too small to be observed at future experiments if models have to accommodate for the relic density measured by WMAP and explain the $(g-2)_\mu$ anomaly: better prospects are found if these two constraints are applied only as upper bounds. The spin-independent neutralino-nucleon cross section in the studied constrained parameter space is just below the present CDMS limit and the running XENON100 experiment will cover the region of the parameter space where the lightest neutralino has large gaugino-higgsino mixing.

PACS numbers: 11.30.Fs, 11.30.Pb, 12.60.Jv, 14.80.Ly, 14.80.Cp

I. INTRODUCTION

One of the appealing features of the minimal supersymmetric standard model (MSSM) with R-parity conservation is the presence of a neutral, stable particle, the lightest neutralino, which presents all the characteristics to be a possible candidate for accounting for the cold dark matter in the Universe [1]. The amount of dark matter Ωh^2 , where Ω is the dark matter density normalized to the critical density of the Universe and h is the reduced Hubble constant, recently has been precisely measured by the WMAP experiment [2].

The Higgs sector of the MSSM [3], especially the heavy neutral Higgses A and H , play a prominent role in the physics of neutralino dark matter in two ways. In some region of the supersymmetric (SUSY) parameter space neutralinos yield the desired amount of relic density by annihilating into fermions through the s -channel resonant exchange of neutral Higgs bosons h , H , A , the so called funnel region where $m_A \simeq 2m_\chi$. As dark matter is expected to be distributed in a halo surrounding our galaxy, neutralinos can scatter off nuclei in terrestrial detectors: coherent scattering is mediated by scalar interactions through the s -channel exchange of squarks and t -channel exchange of the CP-even neutral Higgs bosons h and H . These effects become sizeable when squarks are heavy and $\tan\beta$ is large in reason of the enhanced Higgs bosons coupling to down-type fermions, especially for the b quark which has the largest Yukawa coupling: moreover this couplings receive large radiative SUSY-QCD corrections at large $\tan\beta$ that can be relevant for their production in hadron-hadron collisions at TEVATRON and LHC [4–6]. In this scenario it is well known that B -mesons physics observables are very sensible to Higgs physics [7–11] and put strong constraints on the

parameter space. The branching ratios for τ lepton flavor violating decays are also enhanced near the experimental bounds [12–21, 24–26].

Once a source of LFV is present in the slepton mass matrix, for example the MSSM with the celebrated see saw mechanism for generation of small neutrino masses, two different mechanisms of LFV arise: gauge-mediated LFV effects through the exchange of gauginos and sleptons [29–31] and Higgs-mediated LFV effects through effective non-holomorphic Yukawa interactions for quarks and leptons [7, 12]. LFV Yukawa couplings of the type $\bar{L}_R^i L_L^j H_u^*$ are induced at loop level and become particularly sizable at large $\tan\beta$. In this case the effective flavor-violating Yukawa interactions are described by the lagrangian:

$$-\mathcal{L} \simeq (2G_F^2)^{1/4} \frac{m_{l_i}}{\cos^2\beta} \left(\Delta_{L_L}^{ij} \bar{l}_R^i l_L^j + \Delta_{L_R}^{ij} \bar{l}_L^i l_R^j \right) \times (\cos(\beta - \alpha)h - \sin(\beta - \alpha)H - iA) + h.c. \quad (1)$$

where α is the mixing angle between the CP-even Higgs bosons h and H , A is the physical CP-odd boson, i, j are flavor indices that in the following are understood to be different ($i \neq j$). The coefficients Δ^{ij} in Eq. (1) are induced at one loop level by the exchange of gauginos and sleptons, provided a source of slepton mixing is present. The expressions of $\Delta_{L,R}^{ij}$ in the mass insertion approximation are given by [21]:

$$\Delta_{L_L}^{ij} = -\frac{g'^2}{16\pi^2} \mu m_1 \delta_{LL}^{ij} m_L^2 \times \left[I'(m_1^2, m_R^2, m_L^2) + \frac{1}{2} I'(m_1^2, \mu^2, m_L^2) \right] + \frac{3}{2} \frac{g^2}{16\pi^2} \mu m_2 \delta_{LL}^{ij} m_L^2 I'(m_2^2, \mu^2, m_L^2),$$

$$\Delta_R^{ij} = \frac{g'^2}{16\pi^2} \mu m_1 m_R^2 \delta_{RR}^{ij} [I'(m_1^2, \mu^2, m_R^2) - (\mu \leftrightarrow m_L)] \quad (2)$$

where g and g' are the $SU(2)_L$ and $U(1)_Y$ couplings respectively, μ is the Higgs mixing parameter, $m_{1,2}$ the gaugino mass parameters and $m_{L(R)}^2$ stands for the left-left (right-right) slepton mass matrix entry. I' is the derivative $dI(x, y, z)/dz$ of the three point one-loop integral. The LFV mass insertions $\delta_{LL}^{ij} = (m_L^2)^{ij}/m_L^2$, $\delta_{RR}^{ij} = (m_R^2)^{ij}/m_R^2$, where $(m_{L,R}^2)^{ij}$ are the off-diagonal flavor changing entries of the slepton mass matrix, are free parameters which allow for a model independent study of LFV signals.

The connection between gaugino-mediated LFV signals and neutralino dark matter in the see-saw mechanism implemented in mSUGRA constrained MSSM has been recently studied in Refs. [22, 23]: here it is shown that large neutrino Yukawa coupling affects the renormalization group evolution equations of SUSY parameters from the grand unification (GUT) scale to the electroweak scale (in a $SO(10)$ GUT scenario) enhancing some LFV rates by orders of magnitude and changing also the neutralino relic density and direct and indirect detection rates.

In this paper, on the other hand, we follow a different phenomenological approach: the study is done in the framework of MSSM with real parameters assigning the value of the parameters at the weak scale without any assumption on the mechanism of SUSY breaking or the high energy theory, nor on the origin of LFV entries in the slepton mass matrix and limitate our attention to Higgs mediated flavor violating effects. We study the interplay between the assumptions of the lightest neutralino as dark matter candidate and Higgs mediated flavor violation both to constrain the MSSM parameter space and to give prediction for the neutralino-nucleus scattering and LFV signals at colliders and in τ decays. For related studies see [6, 27, 28].

In Section II we discuss the scan of the parameter space in the real MSSM and the imposed constraints. Then we study their effects on the spin-independent neutralino-nucleon cross section and the arising correlations between supersymmetric parameters in Sec. III. In Section IV we analyse LFV signals $\tau \rightarrow \mu\eta$, $\tau \rightarrow \mu\gamma$, $pp \rightarrow \Phi \rightarrow \tau\mu + X$ at LHC and $\gamma\gamma \rightarrow \tau\mu b\bar{b}$ at a future photon collider. Conclusions are given in Sec. V.

II. CONSTRAINED PARAMETER SPACE

We introduce LFV in the model through the mass insertions $\delta_{LL,RR}^{32} = 0.5$. This value ensures the largest rates in LFV processes and allow us to study the more optimistic scenarios; higher values contradict the mass insertion approximation as an expansion of propagators in these small parameters. Higgs mediated effects become eneteresting at large μ and $\tan\beta$ and low m_A ; further, if SUSY-QCD particles are heavy Higgs effects are dom-

inant also for neutralino dark matter. We thus scan the following real MSSM parameter space:

- $100 \text{ GeV} \leq m_A \leq 1 \text{ TeV}$;
- $20 \leq \tan\beta \leq 60$;
- $500 \text{ GeV} \leq \mu \leq 5 \text{ TeV}$;
The sign of μ is taken positive, as preferred by the SUSY explanation of the $(g-2)_\mu$ anomaly.
- $150 \text{ GeV} \leq m_1, m_2 \leq 1.5 \text{ TeV}$;
We do not impose any relation but let them vary independently. To have large masses for gluinos we choose:
 $1 \text{ TeV} \leq m_3 \leq 5 \text{ TeV}$.
- $1 \text{ TeV} \leq m_{U_3}, m_{D_3}, m_{Q_3} \leq 5 \text{ TeV}$;
for the third generation of squarks: these are varied freely without imposing any relation. For the first and the second generation the soft masses are set to be equal, $m_{U_i} = m_{D_i} = m_{Q_i} = m_{\bar{q}}$, where $i = 1, 2$ and $m_{\bar{q}}$ is another free parameter which varies in the same range.
- $300 \text{ GeV} \leq m_{L_3}, m_{E_3} \leq 2.5 \text{ TeV}$;
for sleptons of the third generation which are independent parameters. For the first and the second generation the soft masses are set to be equal, $m_{L_i} = m_{E_i} = m_{\bar{\ell}}$, where $i = 1, 2$ and $m_{\bar{\ell}}$ is another free parameter which varies in the same range. Sleptons, differently from squarks, can be light in order to explain the $(g-2)_\mu$ anomaly.
- $-2 \leq \frac{AU_3}{m_{U_3}}, \frac{AD_3}{m_{D_3}}, \frac{AE_3}{m_{E_3}} \leq 2$;
for first and second generation the trilinear scalar couplings are set to zero.

The outlined (16-dimensional) large parameter space is restricted imposing the following experimental limits:

- *Light Higgs and SUSY masses.*
LEP, TEVATRON bounds on sparticle masses and the LEP bound on light Higgs: $m_h \geq 114.4 \text{ GeV}$ [32].
- *B-physics observables.*
For the B -physics observables we use the theoretical and experimental numbers of Table 1 in Ref. [33]. Thus we require $0.995 \leq \frac{\mathcal{B}^{MSSM}(B \rightarrow X_s \gamma)}{\mathcal{B}^{SM}(B \rightarrow X_s \gamma)} \leq 1.239$, the upper bound on rare decays $B_s \rightarrow \mu^+ \mu^-$ branching ratio is set to $\mathcal{B}(B_s \rightarrow \mu^+ \mu^-) \leq 4.7 \times 10^{-8}$ and $0.60 \leq \frac{\Delta m_{B_s}^{MSSM}}{\Delta m_{B_s}^{SM}} \leq 1.24$. Finally we require $0.85 \leq \frac{\mathcal{B}^{MSSM}(B \rightarrow \tau \nu)}{\mathcal{B}^{SM}(B \rightarrow \tau \nu)} \leq 1.65$.¹

¹ There is at present a discrepancy between the SM value and the experimental value of the purely leptonic decays branching ratio

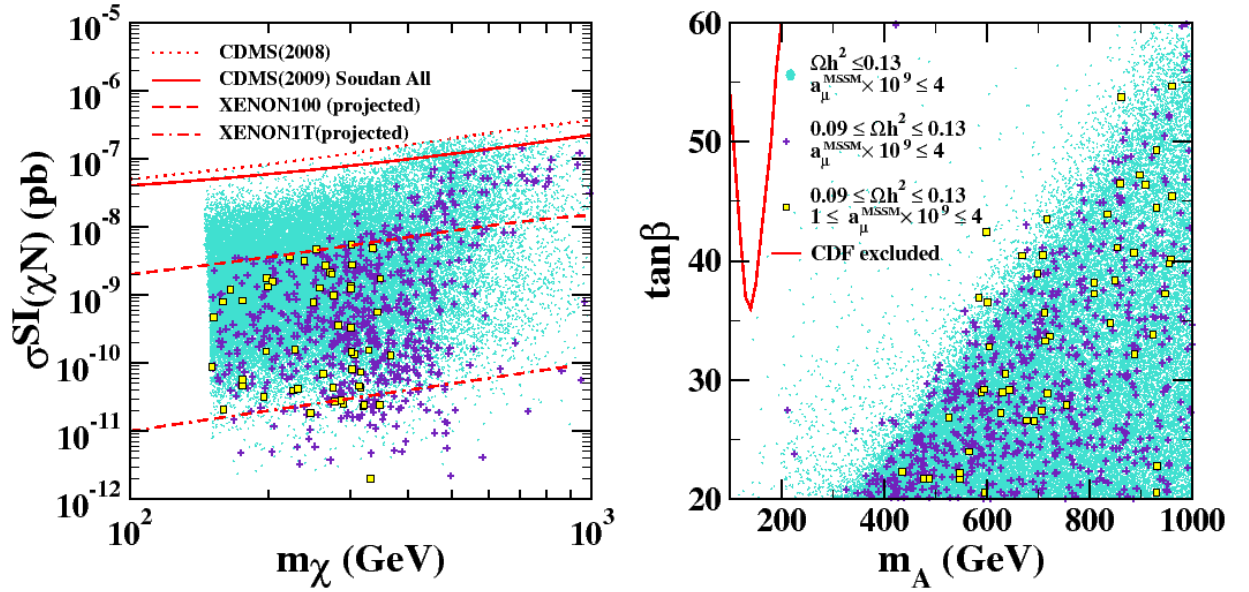


FIG. 1. *Left*: Scatter plot for the spin-independent neutralino-nucleon cross section versus the neutralino mass. The area above the solid line is excluded by the CDMS final results; the area above the dotted line is excluded by the 2008 CDMS search. The dashed and dot-dashed lines give the sensitivity reach of two phases of the XENON experiment. The scanned parameter space and the imposed experimental constraints are described in Sec. II. The different graphical presentation of points corresponds to different steps in imposing the constraints on the $(g-2)_\mu/2$ and on the relic density as explained in the legend of right panel. *Right*: Scatter plot in the $(m_A, \tan\beta)$ plane. The region delimited by the line is excluded by the CDF experiment.

- *LFV τ decays.*

Once Higgs mediated LFV effects are present in the model the non-observation of these rare decays puts strong constraints on the parameter space. The present experimental upper bounds are: $\mathcal{B}(\tau \rightarrow \mu\gamma) \leq 4.4 \times 10^{-8}$ [35], $\mathcal{B}(\tau \rightarrow \mu\eta) \leq 5 \times 10^{-8}$ [44], $\mathcal{B}(\tau \rightarrow \mu\mu\mu) \leq 3.2 \times 10^{-8}$ [44].

- *Relic density.*

We use the conservative WMAP 3σ interval $0.09 \leq \Omega h^2 \leq 0.13$ [2] on the relic density, both applying only the upper limit, (allowing for other sources of dark matter besides the neutralino) and the complete interval. See the legend of Figure 1.

- *Muon anomalous magnetic moment.*

The present discrepancy between $a_\mu^{SM} = (g-2)^{SM}/2$ and the experimental measured value, $\Delta a_\mu = a_\mu^{exp} - a_\mu^{SM}$, lies in the interval $(2-4) \times 10^{-9}$ [36]. We always require $a_\mu^{MSSM} = (g-2)^{MSSM}/2 \leq 4 \times 10^{-9}$. We further show the models which satisfy also the conservative limit lower bound $a_\mu^{MSSM} \geq 1 \times 10^{-9}$. See the legend of Figure 1.

- *Direct dark matter detection.*

The most stringent limit up to date in the neutralino mass range 100 – 1000 GeV for the neutralino-nucleus spin independent cross section comes from the CDMS experiment. The upper limits from the 2008 analysis [37] and the recent final combined results [38] are reported in Fig. 1 (left panel).

- *Non-standard Higgs search at TEVATRON.*

Recently CDF collaboration has published the most stringent exclusion limits in the $(m_A, \tan\beta)$ plane in the light of negative results in the search for heavy neutral Higgs bosons in the inclusive A, H production and the successive decay into $\tau^+\tau^-$ pairs [39]. The excluded region is limited in the low m_A , high $\tan\beta$ region and is depicted in Fig. 1 (right panel).

For numerical computations we use the code DARKSUSY [40] for accelerator bounds, the neutralino relic density and direct dark matter detection in our general MSSM. DARKSUSY uses the code FEYNHIGGS [41] for SUSY and Higgs mass spectrum and Higgs widths and branching ratios. For $b \rightarrow s\gamma$ we used the routines in DARKSUSY while for MSSM contribution to the muon anomalous magnetic moments $(g-2)_\mu$ those of FEYNHIGGS which include also the leading and sub-leading two-loop contributions. For the others B -physics observables we used the formulas of Refs. [10, 11]. We

$\mathcal{B}(B \rightarrow \tau\nu)$ due to a recent analysis [34]. Given the unclear situation both on the theoretical and experimental side we do not consider it here.

generate 10^6 random models, selecting the ones which evade the listed constraints. All of them are applied at the same time with the exception of the relic density and $(g-2)_\mu$ anomaly for which we also relax the lower bounds: thus requiring only $\Omega_\chi h^2 \leq 0.13$ and $a_\mu^{SSM} \leq 4 \times 10^{-9}$ around 4×10^4 survive, the light grey (turquoise) points in the Figures. Requiring also $\Omega_\chi h^2 \geq 0.09$ around 7×10^2 are left, the plus-shaped points, finally if $a_\mu^{SSM} \geq 1 \times 10^{-9}$ only 52 remain, (the square points).

III. NEUTRALINO DARK MATTER

The spin-independent neutralino-nucleon cross section in the limit of heavy squarks and large $\tan\beta$ can be approximated as [4–6, 28]

$$\sigma^{SI} \simeq \frac{g'^2 g^2 |N_{11}|^2 |N_{13}|^2 m_N^4}{4\pi m_W^2 m_A^4} \tan^2 \beta \times K_f, \quad (3)$$

where N_{11} and N_{13} are the lightest neutralino unitary mixing matrix elements, m_N the nucleon mass (neglecting the mass difference between the neutron and the proton) and K_f a factor which depends on nucleon form factors. It scales like $\tan^2 \beta / m_A^4$ and it is able to constrain the low m_A -high $\tan\beta$ region even if to a lesser extent than flavor physics observables that scale like $\tan^6 \beta / m_A^4$.

The right panel of Fig. 1 presents the allowed region in the $(m_A, \tan\beta)$ plane: the region delimited by the line is excluded by CDF search in the channel $p\bar{p} \rightarrow A + X, A \rightarrow \tau^+ \tau^-$. The left panel of Fig. 1 shows the scatter plot for the spin-independent neutralino-nucleon cross section as a function of m_χ and the region excluded by CDMS [37, 38]. We emphasize that CDF and CDMS limits are very mild constraints as can be seen in Fig. 1. The region excluded by CDF is practically excluded by the other constraints while the CDMS limit exclude only one plus-shaped point (not reported in Fig. 1) leaving untouched the regions preferred by WMAP and the $(g-2)_\mu$ anomaly. Further, the final CDMS upper limits curve exclude around 300 light-gray (magenta) points between the solid and the dotted line in Fig. 1 and it is not still constraining the more interesting region. For clarity, in all the other plots only the final CDMS limits are applied. Actually, it is more meaningful to compare the CDMS results with the plus-shaped and square points: in fact the limit on scattering with nuclei are extracted from rates which depend on the local density of dark matter in our galaxy halo which is assumed to be furnished by the weakly interacting massive particle, in this case the lightest neutralino. From this point of view the negative results of these experiments are natural in the present scenario and the two events found in the signal region by CDMS collaboration cannot be explained by our scenario.

The XENON100 experiment [42] should reach the sensitivity corresponding to the dashed gray (red) line in the

Figure 1 (left panel). Such sensitivity is able to cover the region with the highest cross section, $m_\chi \geq 300$ GeV, where there is large higgsino component, as we will discuss below. On the other hand the region preferred by $(g-2)_\mu$ anomaly cannot be covered. We also report the prospected sensitivity goal of the XENON experiment with 1 ton detector mass [42], dot-dashed grey (red) line, which is $10^{-11} - 10^{-10}$ pb for neutralino mass in the range 100 – 1000 GeV: practically all of the parameter space will be probed.

As no relation has been imposed between the neutralino mass and m_A and between gaugino mass parameters, it is interesting to explore which correlations may emerge by the imposition of all the applied constraints.

Fig. 2, left panel, presents the scatter plot of the ratio m_A/m_χ versus m_R/m_χ where m_R is right-right mass parameter for the stau. Points with the correct relic density abundance accumulate along the line $m_A/m_\chi \simeq 2$ where neutralino pair annihilation into fermions through resonant s -channel exchange of neutral Higgs bosons A, H is the dominant mechanism in large portion of the parameter space. Stau coannihilation is at work for models where $m_R \sim m_\chi$ and coannihilation with the second neutralino and the lightest chargino are important for larger values of the ratios.

In the right panel of Fig. 2 the gaugino fraction $|N_{11}|^2 + |N_{12}|^2$ is plotted against the neutralino mass. For neutralino masses below 400 GeV, the preferred region by the $(g-2)_\mu$, is pure gaugino while for masses greater than 400 GeV higgsino component is present. This effect can be seen in Fig. 1 in the spin-independent neutralino cross section which depends on N_{13} ($|N_{13}|^2 + |N_{14}|^2 = 1 - |N_{11}|^2 + |N_{12}|^2$): the models with the highest cross section are the ones with $m_\chi \geq 400$ GeV where the $\chi\chi\Phi$ coupling is enhanced in reason of a larger higgsino component.

The left and right panels of Fig. 3 present the scatter plot in the $(\mu/m_1, m_2/m_1)$ and $(\mu/m_2, m_2/m_1)$ planes respectively. We see that models with the correct relic abundance have $m_2 \geq m_1$ $\mu \geq m_1$. The $(g-2)_\mu$ prefer models with $\mu \geq m_2$. The models with strong gaugino-higgsino mixing, $m_1 \simeq \mu$, $\mu \leq m_2$, $|N_{11}|^2 + |N_{12}|^2 \leq 0.9$ can be probed by XENON100. We further note that most of the point in WMAP and $(g-2)_\mu$ ranges are characterized by having high degeneracy in the gaugino masses $m_1 \simeq m_2$. Such conditions give a “well-tempered bino/wino” neutralino which can be realized in model with split supersymmetry as shown for example in Ref. [43]

IV. PROSPECTS FOR LFV SIGNALS

The τ LFV τ decay which is more sensible to Higgs mediated effects is $\tau \rightarrow \mu\eta$ [13, 16, 18, 20, 24–26] and the

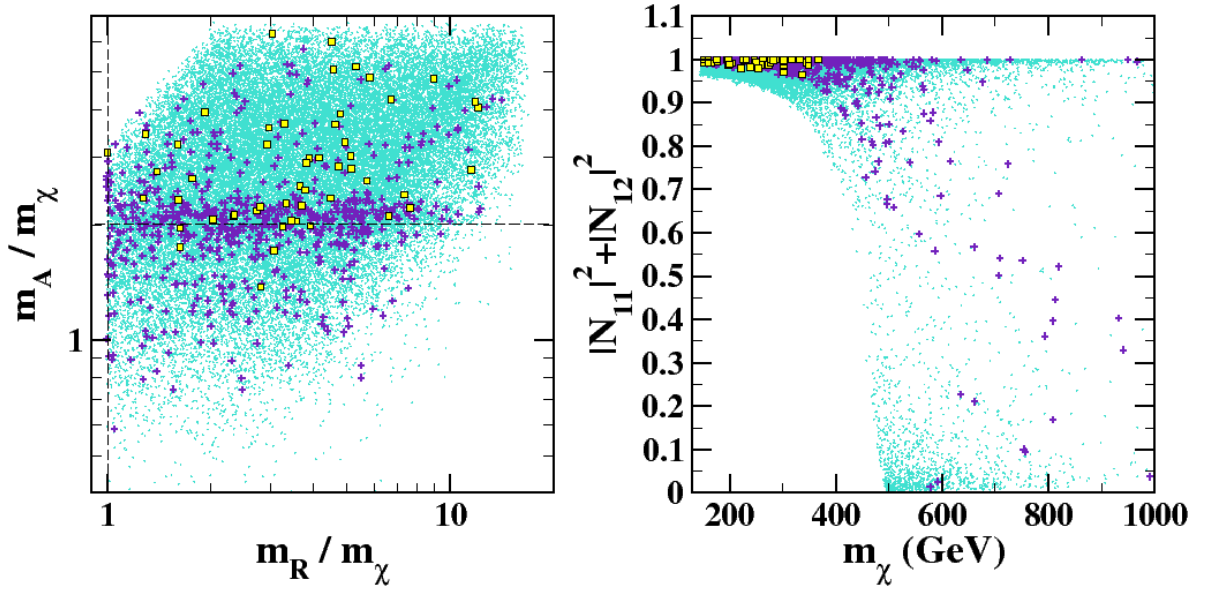


FIG. 2. *Left*: Scatter plot of the ratio m_A/m_χ versus the ratio m_R/m_χ . *Right*: Scatter plot of the gaugino fraction $|N_{11}|^2 + |N_{12}|^2$ versus the neutralino mass. The scanned parameter space and the imposed experimental constraints are described in Sec. II. The same legend of Fig. 1 applies.

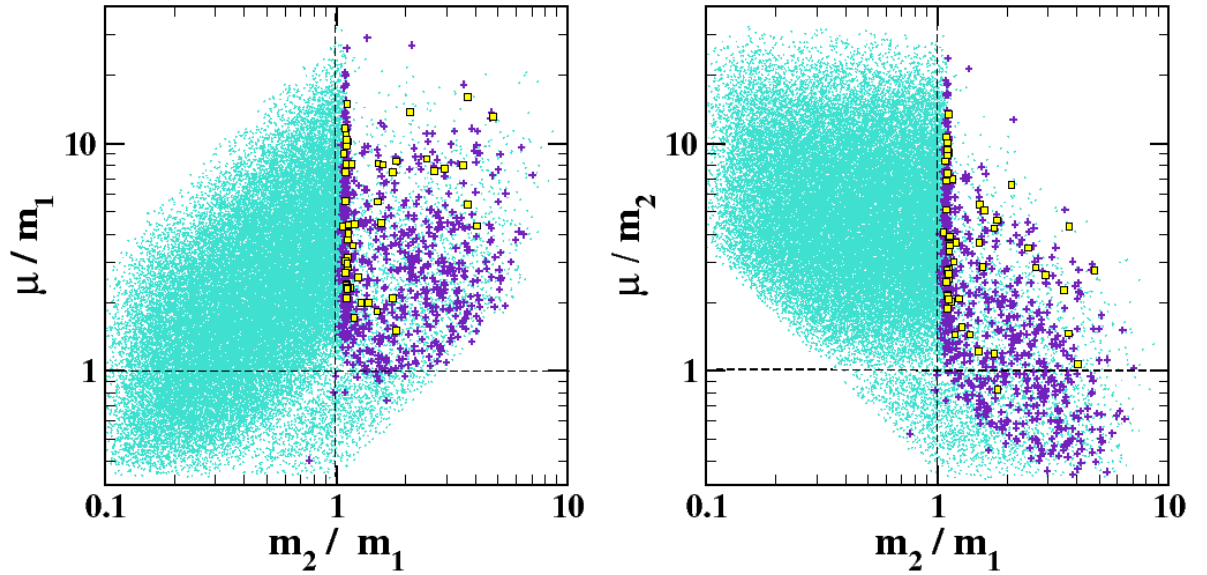


FIG. 3. *Left*: Scatter plot of the ratio μ/m_1 versus m_2/m_1 . *Right*: Scatter plot of the ratio μ/m_2 versus m_2/m_1 . The scanned parameter space and the imposed experimental constraints are described in Sec. II. The same legend of Fig. 1 applies.

branching ratio reads [16, 20]:

$$\frac{\mathcal{B}(\tau \rightarrow \mu\eta)}{\mathcal{B}(\tau \rightarrow \mu\nu\bar{\nu})} = 9\pi^2 \frac{f_\eta^2 m_\eta^4}{m_\tau^2 m_A^4} F_\eta^2 \left(1 - \frac{m_\eta^2}{m_\tau^2}\right)^2 \Delta^2 \tan^6 \beta. \quad (4)$$

Here $f_\eta \simeq 110$ MeV, $\mathcal{B}(\tau \rightarrow \mu\nu\bar{\nu}) = \frac{G_F^2 m_\tau^5}{192\pi^3} \frac{1}{\Gamma}$ and F_η a factor which depends on the hadronisation of quarks bilinears matrix elements: in the treatment of Ref. [16]

it is such that $F_\eta^2 \sim 2.2$. Lepton flavor violation enters through the factor

$$\Delta^2 = |\Delta_L^{32}|^2 + |\Delta_R^{32}|^2. \quad (5)$$

² The approach using chiral perturbation theory [17, 26] gives results different at most by a factor two. These uncertainties will not change our conclusions.

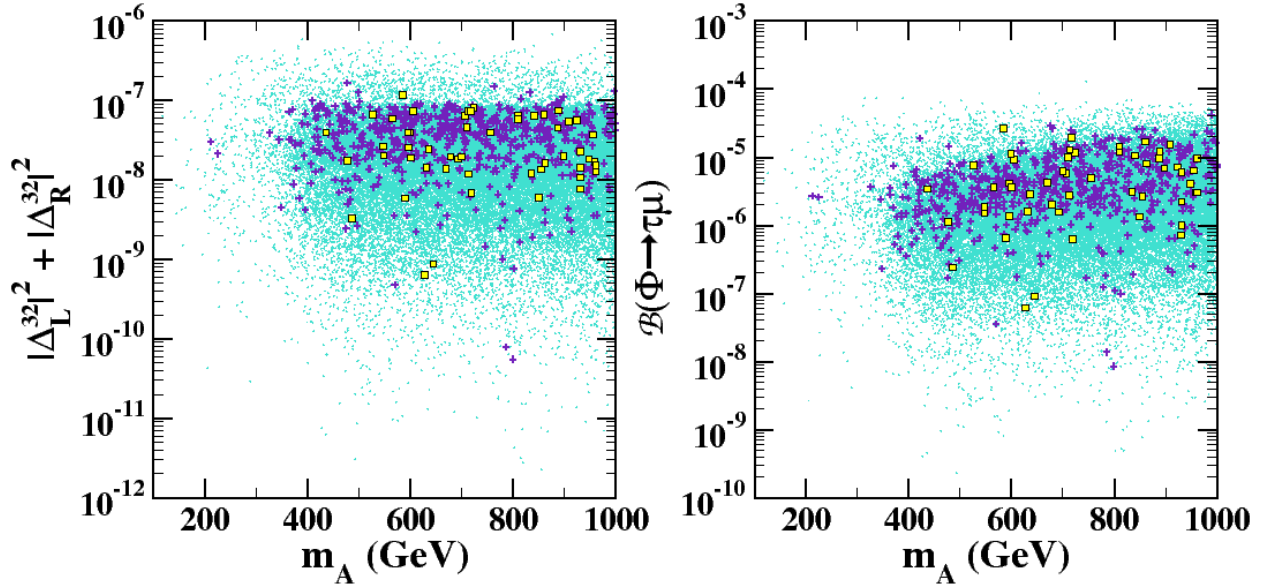


FIG. 4. *Left*: Scatter plot of the LFV violating vertex in Eq. (5) as a function of m_A . *Right*: Scatter plot of the branching ratio $\Phi \rightarrow \tau\mu$ versus m_A ($\Phi = A, H$). The scanned parameter space and the imposed experimental constraints are described in Sec. II. The same legend of Fig. 1 applies.

We also consider the radiative decay $\tau \rightarrow \mu\gamma$ which receives also important contributions by gaugino-slepton loop diagrams: the factors $|\Delta_L^{32}|^2$ and $|\Delta_R^{32}|^2$ enter separately in the branching ratio and not through the combination in Eq. (5). For the computation we used the formulas in Ref. [21] including both gaugino mediated and Higgs mediated effects.

The CP-odd Higgs boson decay width and branching ratio are [46]

$$\begin{aligned} \Gamma(A \rightarrow \tau^+ \mu^-) &= \frac{1}{2} \tan^2 \beta \Delta^2 \Gamma(A \rightarrow \tau^+ \tau^-), \\ \mathcal{B}(A \rightarrow \mu^+ \tau^-) + \mathcal{B}(A \rightarrow \mu^- \tau^+) &= \tan^2 \beta \Delta^2 \mathcal{B}(A \rightarrow \tau^+ \tau^-), \end{aligned} \quad (6)$$

where Δ^2 is defined in Eq. (5) and we used the fact that $\Gamma(A \rightarrow \tau^+ \mu^-) = \Gamma(A \rightarrow \tau^- \mu^+)$. For the CP-even Higgs boson H , the right hand sides of Eq. (6), are multiplied by a factor $\sin(\beta - \alpha)/(\cos \alpha)^2$ which is order one in our scenario where $m_A \simeq m_H$, thus the previous formulas hold for both bosons.

In Fig. IV, left panel, we present the scatter plot for the effective vertex given by Eq. (5), while the right panel shows the scatter plot of the branching ratio given by Eq. (6) as a function of m_A . We see that they reach 10^{-7} and 3×10^{-5} respectively for models preferred by WMAP measurements, two orders of magnitude lower than what found without imposing it on the parameter space [15, 45, 46]. The branching ratios of LFV decays $\tau \rightarrow \mu\eta$ and $\tau \rightarrow \mu\gamma$ versus m_A are given in Fig. 5. For models with the correct neutralino relic density abundance and preferred by the $(g - 2)_\mu$ anomaly, both are generally under 10^{-10} while relaxing the constraints lower bound they can reach the 10^{-9} level. We remind

that at a Super-B factory the present limits $\mathcal{O}(10^{-8})$ can be lowered to $\mathcal{O}(10^{-9} \sim 10^{-10})$ for the $\mu\eta$ final state because the branching ratio scales linearly with the luminosity due to practically negligible background. In the $\mu\gamma$ case for the presence of large background the branching ratio scale as the square root of the luminosity and the sensitivity reach is one order of magnitude lower [44].

We further revisit the prospects for detection of Higgs LFV signals in pp collisions at LHC [15, 45] and in $\gamma\gamma$ collisions at the photon collider option of the future International Linear Collider [46].

At high $\tan \beta$ the dominant production mechanisms for A, H at LHC is $b\bar{b}$ fusion due to the $m_b \tan \beta$ enhanced $b\bar{b}\Phi$ couplings. We calculate the cross section with FEYNHIGGS which uses the approximation

$$\sigma^{MSSM}(b\bar{b} \rightarrow \Phi) = \sigma^{SM}(b\bar{b} \rightarrow \Phi) \frac{\Gamma(\Phi \rightarrow b\bar{b})^{MSSM}}{\Gamma(\Phi \rightarrow b\bar{b})^{SM}}, \quad (7)$$

where $\sigma^{SM}(b\bar{b} \rightarrow \Phi)$ is the total SM cross section for production of Higgs boson with mass m_Φ via $b\bar{b}$ fusion: to obtain the value in the MSSM it is rescaled with the ratio of the decay width of the inverse process in the MSSM over the SM decay width [41, 48, 49]. We calculate for each random model the product the $\sigma(pp \rightarrow \Phi + X) \times \mathcal{B}(\Phi \rightarrow \tau\mu)$. As masses and couplings of A and H are practically identical as discussed above, we have $\sigma(pp \rightarrow A + X) + \sigma(pp \rightarrow H + X) \simeq 2\sigma(pp \rightarrow A + X)$.

The scatter plot $\sigma(pp \rightarrow \Phi + X) \times \mathcal{B}(\Phi \rightarrow \tau\mu)$ is shown in Fig. 6, left panel. We see that with the nominal integrated luminosity of 100 fb^{-1} per year models which satisfy both the relic density abundance and Δa_μ can give up to 10 events per year (squared points), up to 40

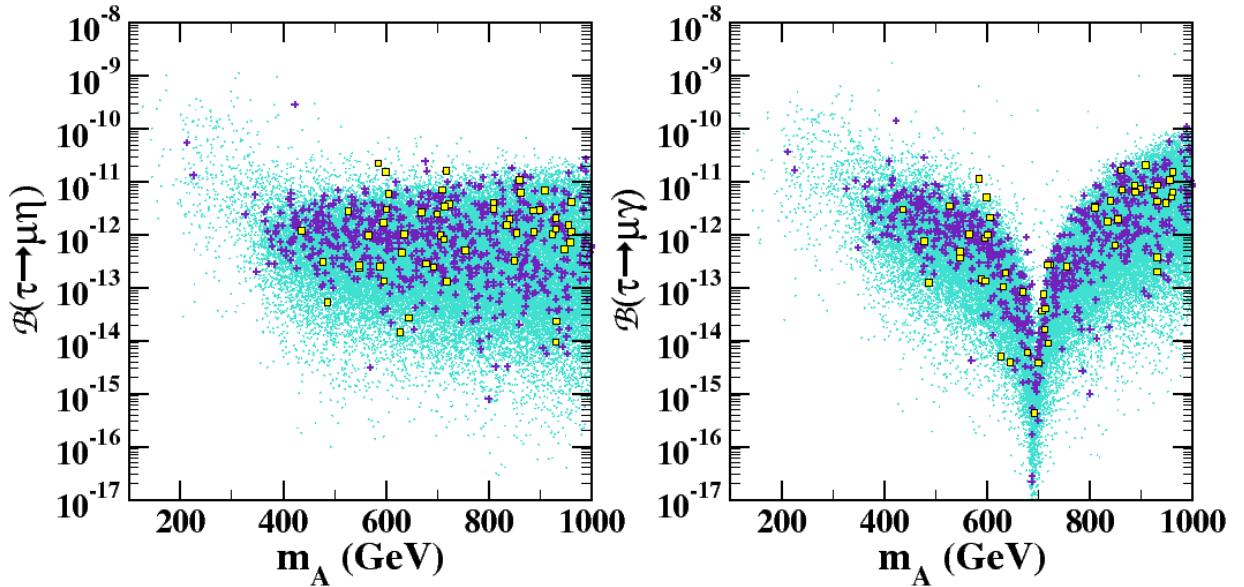


FIG. 5. *Left:* Scatter plot of the LFV violating vertex in Eq. (5) as a function of m_A . *Right:* Scatter plot of the branching ratio $\Phi \rightarrow \tau\mu$ versus m_A ($\Phi = A, H$). The scanned parameter space and the imposed experimental constraints are described in Sec. II. The same legend of Fig. 1 applies.

if we relax the condition on the lower limit of Δa_μ (plus-shaped points) and up to 200-300 relaxing both the lower limits (magenta (grey) points).

In $\gamma\gamma$ collisions the main production mechanism for $\Phi = A, H$ is $\tau\tau$ fusion [47] while the $b\bar{b}$ is suppressed by a factor $3(1/3)^4(m_b/m_\tau)^2 \simeq 0.1$ which cannot be compensated by corrections to the b Yukawa coupling. In Ref. [46] we studied in detail the $\mu\tau$ fusion process $\gamma\gamma \rightarrow \mu\tau b\bar{b}$ where the Higgs boson is produced in the s -channel via a virtual $\mu\tau$ pair and can be detected from its decay mode $A \rightarrow b\bar{b}$.

A good analytical approximation for the cross section is obtained using the equivalent particle approximation wherein the colliding real photons split respectively into τ and μ pairs with the subsequent $\mu\tau$ fusion into the Higgs boson. The splitting functions of the photon at leading order read [47]:

$$P_{\gamma/\ell}(x) = \frac{\alpha}{2\pi} [x^2 + (1-x)^2] \ln \left(\frac{m_\Phi^2}{m_\ell^2} \right), \quad (8)$$

thus the cross section is given by:

$$\sigma(\gamma\gamma \rightarrow \mu\tau b\bar{b}; s_{\gamma\gamma}) = \frac{4\pi^2}{s_{\gamma\gamma}} \frac{\Gamma(A \rightarrow \tau\mu) \mathcal{B}(A \rightarrow b\bar{b})}{M_A} \times 2 \int_{-\ln 1/t}^{+\ln 1/t} d\eta P_{\gamma/\mu}(te^\eta) P_{\gamma/\tau}(te^{-\eta}), \quad (9)$$

with $t = m_A/2E_\gamma$, $\eta = \ln \sqrt{x_\mu/x_\tau}$, x is the fraction of the energy of the photon carried by the virtual lepton. In [46] we have shown that the effect of photons spectra can be neglected, we thus consider monochromatic photons with

$\sqrt{s_{\gamma\gamma}} = 600$ GeV, and photon-photon luminosity $500 \text{ fb}^{-1} \text{ yr}^{-1}$ based on the parameters of TESLA(800) [50].

The scatter plot of the signal cross section versus m_A is shown in Fig. 6, right panel. Here the models which satisfy both the relic density abundance and Δa_μ (squared points) have maximal cross section 10^{-3} fb , which is too small. Relaxing the lower limits cross section values up to $2 \times 10^{-2} \text{ fb}$ are possible, giving 10 events/year.

V. SUMMARY AND CONCLUSIONS

In the framework of the MSSM with heavy SUSY-QCD particles and large $\tan \beta$ we have studied lepton flavor violation mediated by the heavy neutral Higgs $\Phi = A, H$ in $\tau-\mu$ sector both in τ lepton decays, $\tau \rightarrow \mu\eta$ and $\tau \rightarrow \mu\gamma$, and at high energy collider through the production and decay at LHC, $pp \rightarrow \Phi + X$, $\Phi \rightarrow \tau\mu$ and the $\mu-\tau$ fusion at a photon collider, $\gamma\gamma \rightarrow \tau\mu b\bar{b}$. The approach to LFV has been model independent by the use of the mass insertion approximation. We used large mass insertions $\delta_{LL}^{ij} = \delta_{RR}^{ij} = 0.5$ to estimate the number of events in the most favourable scenario that can be obtained in future experiments. With such a large source of LFV the branching ratios of rare decays can exceed the present experimental upper bounds from BABAR and BELLE which therefore provide constraints on the MSSM parameter space in presence of LFV. Other constraints that have been imposed are limits from direct search of sparticles and of the light Higgs, B -physics observables, the $(g-2)_\mu$ anomaly, and recent limits from TEVATRON search of non standard Higgs bosons in the $\tau\tau$ channel. In

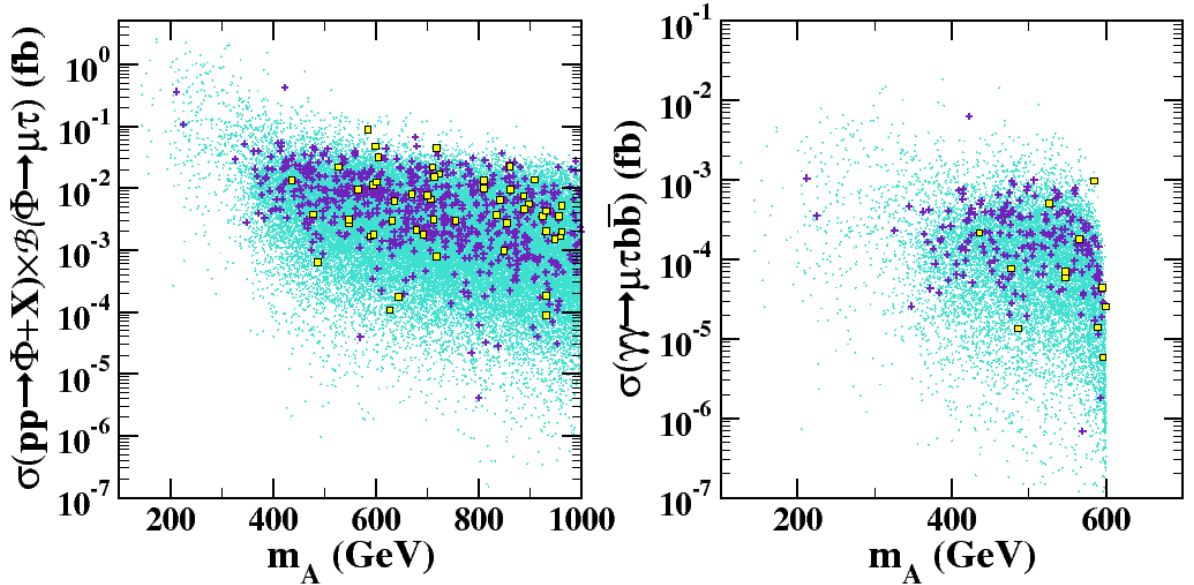


FIG. 6. *Left*: Scatter plot of the inclusive production cross section $pp \rightarrow \Phi + X$ times the branching ratio of $\Phi \rightarrow \tau\mu$ at LHC versus m_A ($\Phi = A, H$). *Right*: Scatter plot for the cross section of the process $\gamma\gamma \rightarrow \tau\mu b\bar{b}$ in photon-photon collision at $\sqrt{s_{\gamma\gamma}} = 600$ GeV. The scanned parameter space and the imposed experimental constraints are described in Sec. II. The same legend of Fig. 1 applies.

the R-parity conserving MSSM the heavy neutral Higgs play an important role both in neutralino annihilation cross sections to satisfy the relic density of dark matter measured by WMAP and in the spin-independent neutralino nucleon cross section in direct dark matter search experiment. We thus have imposed on the MSSM parameter space the present CDMS exclusion limit and the WMAP limits on Ωh^2 .

We have found that in models with $0.09 \leq \Omega_\chi h^2 \leq 0.13$ and $1 \leq a_\mu^{MSSM} \times 10^9 \leq 4$: the branching ratios of $\tau \rightarrow \mu\eta$, $\tau \rightarrow \mu\gamma$ are both under the $\mathcal{O}(10^{-10})$ thus probably undetectable even at super-B factory; at LHC the cross section for $pp \rightarrow \Phi + X$, $\Phi \rightarrow \tau\mu$ can reach $\mathcal{O}(10^{-1} - 10^{-2})$ fb in the range $m_A = 400 - 1000$ GeV giving up to 10 events with 100 fb^{-1} ; the cross section of $\gamma\gamma \rightarrow \tau\mu b\bar{b}$ reach $\mathcal{O}(10^{-3})$ fb, thus too small even for the large value of the expected luminosity of 500 fb^{-1} . Prospects are somewhat more encouraging if we relax the lower limits, imposing only $\Omega_\chi h^2 \leq 0.13$ and $a_\mu^{MSSM} \times 10^9 \leq 4$. In this case branching ratios of LFV τ decays can reach $\mathcal{O}(10^9)$, the cross sections at LHC about 2 fb for low m_A masses and around 2×10^{-2} fb in $\gamma\gamma$ collisions.

We derive two main indications from this analysis. On

one hand, even with large sources of lepton flavor violation in the slepton mass matrix, the process where Higgs mediated $\tau - \mu$ transitions should manifest could be beyond the sensitivity reach of future experiments. On the other hand, to observe such effects, in any case, the full luminosity of the machine is needed.

We emphasize that our not optimistic conclusions are specific to Higgs mediated effects. As shown in [22], in typical SUSY parameter space where gaugino-mediated effects are dominant over Higgs mediated ones and in the context of SUSY see-saw mechanism, LFV rates are detectable by future experiments.

We have also studied the spin-independent neutralino nucleus cross section: we have shown that in models that satisfy $0.09 \leq \Omega_\chi h^2 \leq 0.13$ and $1 \leq a_\mu^{MSSM} \times 10^9 \leq 4$, the cross section lies just below the sensitivity of XENON100 which should report results soon. The full XENON 1 ton is needed to cover all the parameter space. However, if the lower limit on $(g - 2)_\mu$ is not considered XENON100 is sensitive to the neutralino mass range 300-1000 GeV in models where the higgsino component is large.

-
- [1] G. Jungman, M. Kamionkowski and K. Griest, Phys. Rept. **267**, 195 (1996) [arXiv:hep-ph/9506380]; G. Bertone, D. Hooper and J. Silk, Phys. Rept. **405**, 279 (2005) [arXiv:hep-ph/0404175].
 [2] D. N. Spergel *et al.* [WMAP Collaboration], Astrophys.

- J. Suppl. **170**, 377 (2007) [arXiv:astro-ph/0603449].
 [3] A. Djouadi, Phys. Rept. **459**, 1 (2008) [arXiv:hep-ph/0503173].
 [4] M. S. Carena, D. Hooper and P. Z. Skands, Phys. Rev. Lett. **97**, 051801 (2006) [arXiv:hep-ph/0603180].

- [5] M. S. Carena, D. Hooper and A. Vallinotto, Phys. Rev. D **75**, 055010 (2007) [arXiv:hep-ph/0611065].
- [6] M. S. Carena, A. Menon and C. E. M. Wagner, Phys. Rev. D **76**, 035004 (2007) arXiv:0704.1143 [hep-ph].
- [7] K. S. Babu and C. F. Kolda, Phys. Rev. Lett. **84**, 228 (2000) [arXiv:hep-ph/9909476].
- [8] G. Isidori and A. Retico, JHEP **0111**, 001 (2001) [arXiv:hep-ph/0110121].
- [9] G. D'Ambrosio, G. F. Giudice, G. Isidori and A. Strumia, Nucl. Phys. B **645**, 155 (2002) [arXiv:hep-ph/0207036].
- [10] A. J. Buras, P. H. Chankowski, J. Rosiek and L. Slawianowska, Nucl. Phys. B **659**, 3 (2003) [arXiv:hep-ph/0210145].
- [11] G. Isidori and P. Paradisi, Phys. Lett. B **639**, 499 (2006) [arXiv:hep-ph/0605012].
- [12] K. S. Babu and C. Kolda, Phys. Rev. Lett. **89**, 241802 (2002) [arXiv:hep-ph/0206310].
- [13] M. Sher, Phys. Rev. D **66**, 057301 (2002) [arXiv:hep-ph/0207136].
- [14] A. Dedes, J. R. Ellis and M. Raidal, Phys. Lett. B **549**, 159 (2002) [arXiv:hep-ph/0209207].
- [15] A. Brignole and A. Rossi, Phys. Lett. B **566**, 217 (2003) [arXiv:hep-ph/0304081].
- [16] A. Brignole and A. Rossi, Nucl. Phys. B **701**, 3 (2004) [arXiv:hep-ph/0404211].
- [17] E. Arganda, A. M. Curiel, M. J. Herrero and D. Temes, Phys. Rev. D **71**, 035011 (2005) [arXiv:hep-ph/0407302].
- [18] S. Kanemura, T. Ota and K. Tsumura, Phys. Rev. D **73**, 016006 (2006) [arXiv:hep-ph/0505191].
- [19] J. K. Parry, Nucl. Phys. B **760**, 38 (2007) [arXiv:hep-ph/0510305].
- [20] P. Paradisi, J. High Energy Phys. 02, (2006) 050. [arXiv:hep-ph/0508054].
- [21] P. Paradisi, J. High Energy Phys. 08, (2006) 047. [arXiv:hep-ph/0601100].
- [22] V. Barger, D. Marfatia, A. Mustafayev and A. Soleimani, Phys. Rev. D **80**, 076004 (2009) [arXiv:0908.0941 [hep-ph]].
- [23] V. Barger, D. Marfatia and A. Mustafayev, Phys. Lett. B **665**, 242 (2008) [arXiv:0804.3601 [hep-ph]].
- [24] C. H. Chen and C. Q. Geng, Phys. Rev. D **74**, 035010 (2006) [arXiv:hep-ph/0605299].
- [25] E. Arganda, M. J. Herrero and J. Portoles, JHEP **0806**, 079 (2008) [arXiv:0803.2039 [hep-ph]].
- [26] M. J. Herrero, J. Portoles and A. M. Rodriguez-Sanchez, Phys. Rev. D **80**, 015023 (2009) [arXiv:0903.5151 [hep-ph]].
- [27] G. Isidori, F. Mescia, P. Paradisi and D. Temes, Phys. Rev. D **75**, 115019 (2007) [arXiv:hep-ph/0703035].
- [28] M. Carena, A. Menon and C. E. M. Wagner, Phys. Rev. D **79**, 075025 (2009) [arXiv:0812.3594 [hep-ph]].
- [29] F. Borzumati and A. Masiero, Phys. Rev. Lett. **57**, 961 (1986).
- [30] J. Hisano, T. Moroi, K. Tobe, M. Yamaguchi and T. Yanagida, Phys. Lett. B **357**, 579 (1995) [arXiv:hep-ph/9501407].
- [31] J. Hisano, T. Moroi, K. Tobe and M. Yamaguchi, Phys. Rev. D **53**, 2442 (1996) [arXiv:hep-ph/9510309].
- [32] C. Amsler *et al.* [Particle Data Group], Phys. Lett. B **667**, 1 (2008).
- [33] O. Buchmueller *et al.*, Eur. Phys. J. C **64**, 391 (2009) [arXiv:0907.5568 [hep-ph]].
- [34] M. Bona *et al.* [UTfit Collaboration], arXiv:0908.3470 [hep-ph].
- [35] B. Aubert [The BABAR Collaboration], arXiv:0908.2381 [hep-ex].
- [36] K. Hagiwara, A. D. Martin, D. Nomura and T. Teubner, Phys. Lett. B **649** (2007) 173 [arXiv:hep-ph/0611102].
- [37] Z. Ahmed *et al.* [CDMS Collaboration], Phys. Rev. Lett. **102**, 011301 (2009) [arXiv:0802.3530 [astro-ph]].
- [38] Z. Ahmed *et al.* [The CDMS-II Collaboration], arXiv:0912.3592 [astro-ph.CO].
- [39] T. Aaltonen *et al.* [CDF Collaboration], arXiv:0906.1014 [hep-ph].
- [40] P. Gondolo, J. Edsjö, P. Ullio, L. Bergström, M. Schelke and E. A. Baltz, JCAP **0407**, 008 (2004) [arXiv:astro-ph/0406204]. Web page: <http://www.physto.se/~edsjo/darksusy>.
- [41] S. Heinemeyer, W. Hollik and G. Weiglein, Comput. Phys. Commun. **124**, 76 (2000) [arXiv:hep-ph/9812320]. Home page: www.feynhiggs.de.
- [42] E. Aprile, AIP Conf. Proc. **1078**, 530 (2009).
- [43] N. Arkani-Hamed, A. Delgado and G. F. Giudice, Nucl. Phys. B **741**, 108 (2006) [arXiv:hep-ph/0601041].
- [44] Y. Miyazaki [Belle Collaboration], Nucl. Phys. Proc. Suppl. **189**, 148 (2009).
- [45] J. L. Diaz-Cruz, D. K. Ghosh and S. Moretti, Phys. Lett. B **679**, 376 (2009) [arXiv:0809.5158 [hep-ph]].
- [46] M. Cannoni and O. Panella, Phys. Rev. D **79**, 056001 (2009) [arXiv:0812.2875 [hep-ph]].
- [47] S. Y. Choi, J. Kalinowski, J. S. Lee, M. M. Muhlleitner, M. Spira and P. M. Zerwas, Phys. Lett. B **606**, 164 (2005) [arXiv:hep-ph/0404119].
- [48] T. Hahn, S. Heinemeyer, F. Maltoni, G. Weiglein and S. Willenbrock, arXiv:hep-ph/0607308.
- [49] M. S. Carena, S. Heinemeyer, C. E. M. Wagner and G. Weiglein, Eur. Phys. J. C **45**, 797 (2006) [arXiv:hep-ph/0511023].
- [50] B. Badelek *et al.* [ECFA/DESY Photon Collider Working Group], Int. J. Mod. Phys. A **19**, 5097 (2004) [arXiv:hep-ex/0108012].